

# Quadrature-to-directional format conversion of Doppler signals using digital methods

Nizamettin Aydin, Lingke Fan and David H Evans

Division of Medical Physics, Faculty of Medicine, Leicester University, Leicester, UK

Received 12 November 1993

**Abstract.** Four possible quadrature-to-directional format conversion methods using digital techniques are described. These are the phasing-filter technique, the extended Weaver receiver technique, the Hilbert transform in the frequency domain, and the complex FFT. All methods are implemented to give separated time domain outputs as well as frequency domain outputs. The theoretical descriptions are verified by practical implementations. Each of the methods has been implemented in real-time using a commercially available digital signal processing board.

## 1. Introduction

The quadrature detection method which is employed in most Doppler ultrasound systems produces in-phase and quadrature-phase components of the Doppler shift signal. To derive clinical information from this signal, the quadrature Doppler signals must be decoded into the forward and reverse components of flow. A number of directional techniques based on analogue systems have been reviewed by Coghlan and Taylor (1976), and more recently techniques based on digital signal processing (DSP) methods have been described by Aydin and Evans (1994). In both these previous publications the emphasis was on the frequency domain display of the separated Doppler signal, not on their time domain separation. It is sometimes necessary, however, to separate the signals in the time domain, either so that forward and reverse flow can be presented as a stereo pair, or so that the signals may be recorded on to audio tape. The latter is not possible with quadrature signals because neither analogue (Smallwood 1985) nor digital audio tape recorders (Bush and Evans 1993) are capable of preserving the precise phase relationship of the quadrature pair to permit the subsequent separation of the forward and reverse signals.

This paper is concerned with methods for deriving separated forward and reverse signals in the time domain from quadrature Doppler signals using DSP methods. These methods will be presented under two main processing strategies: time domain processing and frequency domain processing.

Each of the methods will be described theoretically, and experimental results using a narrow-band quadrature signal derived from a white-noise generator presented.

## 2. Theory of quadrature-to-directional Doppler signal conversion

In order to generalize the methods defined in this paper, a discrete Doppler quadrature signal pair containing information concerning forward channel and reverse channel signals  $s_f(n)$

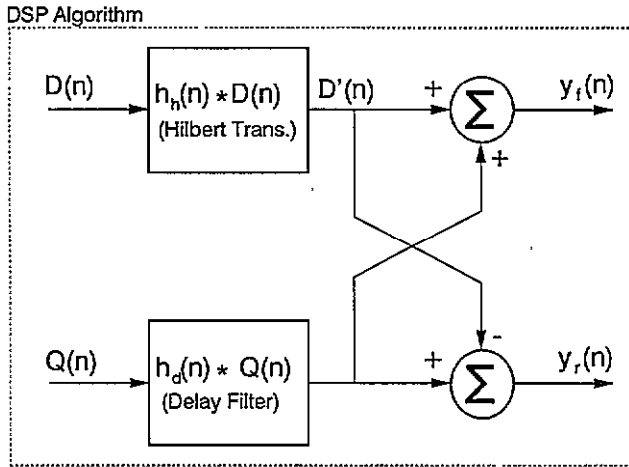


Figure 1. Phasing-filter technique for use with quadrature phase detected signals.

and  $s_r(n)$  will be considered. This signal pair can be generally expressed as

$$\begin{cases} D(n) = s_f(n) + H[s_r(n)] \\ Q(n) = H[s_f(n)] + s_r(n) \end{cases} \quad (1)$$

where  $H[ ]$  stands for the ‘Hilbert transform of’. Since all the methods are implemented digitally, generalizations are made using the discrete form of the signal definition. Unless otherwise stated the Doppler signal pair is band-limited to  $f_s/2$ , where  $f_s$  is the sampling frequency of the system.

As they have no significance on the results, all delays introduced by the digital filters have been ignored.

2.1. Time domain processing

Two types of time domain processing will be presented: the phasing filter technique which is based on the Hilbert transform (HT) implemented using a convolution, and the extended Weaver receiver technique which is based on the quadrature demodulation and frequency translation principles.

2.1.1. Phasing-filter technique (PFT). The algorithm shown in figure 1 is based on a wide-band digital HT. The HT is the name given to an operator which, when applied to a band-limited signal, generates the exact quadrature form of the waveform. A discrete-time HT (Cizek 1970, Gold et al 1970, Oppenheim and Schaffer 1975) is a linear shift-invariant discrete-time system whose ideal frequency response  $H(\omega)$  is given by

$$H(\omega) = \begin{cases} -j, & 0 \leq \omega < \pi \\ +j, & -\pi \leq \omega < 0. \end{cases} \quad (2)$$

The corresponding ideal impulse response is given by

$$h(n) = \begin{cases} \frac{2 \sin^2(\pi n/2)}{\pi n} & n \neq 0 \\ 0 & n = 0. \end{cases} \quad (3)$$

If the signal defined by equation (1) is applied to the system illustrated in figure 1, the following results are obtained.

According to the properties of the HT (Schwartz *et al* 1966), the HT of  $D(n)$  is

$$D'(n) = H[D(n)] = H[s_f(n) + H[s_r(n)]] = H[s_f(n)] - s_r(n). \tag{4}$$

After addition and subtraction of  $Q(n)$  (equation (1)) and  $D'(n)$  (equation (4)) the separated outputs will be

$$\begin{cases} y_f(n) = Q(n) + D'(n) = 2H[s_f(n)] \\ y_r(n) = Q(n) - D'(n) = 2s_r(n) \end{cases} \tag{5}$$

where the outputs are totally separated.

**2.1.2. Extended Weaver receiver technique (EWRT).** The block diagram of this algorithm is shown in figure 2. This method is an extension of the Weaver receiver technique (WRT) described by Aydin and Evans (1994). It uses the frequency conversion or modulation technique. The results at stages X1, Y1 and X2 are the same as for the WRT. Additionally, this method utilizes a low-pass filter (LPF) stage and an extra mixing stage. The last filtering stage is optional since the reconstruction and anti-aliasing filters provide enough attenuation of the unwanted frequency components, which are usually far beyond the cut-off frequency. If the additional filter stage is used, a sharp decline after the cut-off frequency is not necessary.

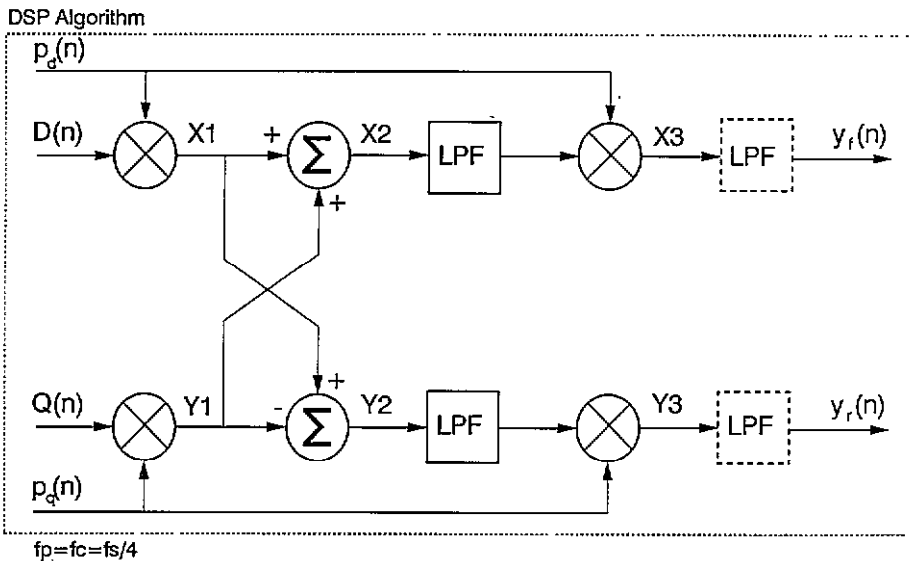


Figure 2. Extended Weaver receiver technique for use with quadrature phase detected signals.

For a theoretical description of the system consider the quadrature Doppler signal defined by equation (1) which is band limited to  $f_s/4$ , and a pair of quadrature pilot frequency signals given by  $p_d(n) = \sin \omega_c n$ ,  $p_q(n) = \cos \omega_c n$  where  $\omega_c/2\pi = f_s/4$ . The LPF is assumed to be an ideal LPF having a cut-off frequency of  $f_s/4$ .

Since the first stage is basically a single side-band (SSB) signal generator, the general expression for this stage (Gibson 1989) is that

$$\begin{aligned} X2, Y2 &= D(n) \times p_d(n) \pm Q(n) \times p_q(n) \\ &= \{s_f(n) \times \sin \omega_c n + H[s_r(n)] \times \sin \omega_c n\} \pm \{H[s_r(n)] \times \cos \omega_c n + s_r(n) \cos \omega_c n\}. \end{aligned} \quad (6)$$

If we define the Fourier transform of  $s_f(n)$  and  $s_r(n)$  as

$$F\{s_f(n)\} = S_f(\omega) \quad \text{and} \quad F\{s_r(n)\} = S_r(\omega) \quad (7)$$

then

$$F\{H[s_f(n)]\} = H[S_f(\omega)] = \begin{cases} -jS_f(\omega) & 0 \leq \omega < \pi \\ +jS_f(\omega) & -\pi \leq \omega < 0 \end{cases} \quad (8)$$

$$F\{H[s_r(n)]\} = H[S_r(\omega)] = \begin{cases} -jS_r(\omega) & 0 \leq \omega < \pi \\ +jS_r(\omega) & -\pi \leq \omega < 0. \end{cases} \quad (9)$$

Defining

$$\begin{cases} S_f^+(\omega) = S_f(\omega) & 0 \leq \omega < \pi \\ S_f^-(\omega) = S_f(\omega) & -\pi \leq \omega < 0 \end{cases} \quad (10)$$

$$\begin{cases} S_r^+(\omega) = S_r(\omega) & 0 \leq \omega < \pi \\ S_r^-(\omega) = S_r(\omega) & -\pi \leq \omega < 0 \end{cases} \quad (11)$$

we can write

$$\begin{cases} S_f(\omega) = S_f^+(\omega) + S_f^-(\omega) \\ S_r(\omega) = S_r^+(\omega) + S_r^-(\omega) \end{cases} \quad (12)$$

$$\begin{cases} H[S_f(\omega)] = -jS_f^+(\omega) + jS_f^-(\omega) \\ H[S_r(\omega)] = -jS_r^+(\omega) + jS_r^-(\omega). \end{cases} \quad (13)$$

Taking the Fourier transform of equation (6), we have

$$\begin{aligned} F\{X2\} &= \{-jS_f^+(\omega - \omega_c) + jS_f^-(\omega + \omega_c)\} + \{S_r^+(\omega + \omega_c) + S_r^-(\omega - \omega_c)\} \\ &= H[S_f(\omega_c - \omega)] + S_r(\omega_c + \omega) \end{aligned} \quad (14)$$

$$\begin{aligned} F\{Y2\} &= \{jS_f^+(\omega + \omega_c) - jS_f^-(\omega - \omega_c)\} + \{-S_r^+(\omega - \omega_c) - S_r^-(\omega + \omega_c)\} \\ &= -H[S_f(\omega_c + \omega)] - S_r(\omega_c - \omega). \end{aligned} \quad (15)$$

If we pass the signal defined by equation (14) and equation (15) through the LPF that retains only the lower side-band, the remaining signals are

$$F\{X2\} = H[S_f(\omega_c - \omega)] = -jS_f^+(\omega - \omega_c) + jS_f^-(\omega + \omega_c) \quad (16)$$

$$F\{Y2\} = -S_r(\omega_c - \omega) = -S_r^+(\omega - \omega_c) - S_r^-(\omega + \omega_c). \quad (17)$$

Similarly, the outputs of the second mixing stage are

$$\begin{aligned} F\{X3\} &= \frac{1}{2}S_f^+(\omega) + \frac{1}{2}S_f^-(\omega) - \frac{1}{2}S_f^+(\omega - 2\omega_c) - \frac{1}{2}S_f^-(\omega + 2\omega_c) \\ &= \frac{1}{2}S_f(\omega) - \frac{1}{2}S_f(2\omega_c - \omega) \end{aligned} \quad (18)$$

$$\begin{aligned} F\{Y3\} &= -\frac{1}{2}S_r^+(\omega) - \frac{1}{2}S_r^-(\omega) - \frac{1}{2}S_r^+(\omega - 2\omega_c) - \frac{1}{2}S_r^-(\omega + 2\omega_c) \\ &= -\frac{1}{2}S_r(\omega) - \frac{1}{2}S_r(2\omega_c - \omega). \end{aligned} \quad (19)$$

Applying the LPF, the frequency components greater than  $f_c$  are removed, so the separated outputs are

$$\begin{cases} F\{y_f(n)\} = \frac{1}{2}S_f(\omega) \\ F\{y_r(n)\} = -\frac{1}{2}S_r(\omega). \end{cases} \quad (20)$$

Taking the inverse Fourier transform of these results, we have

$$\begin{cases} y_f(n) = F^{-1}\{\frac{1}{2}S_f(\omega)\} = \frac{1}{2}s_f(n) \\ y_r(n) = F^{-1}\{-\frac{1}{2}S_r(\omega)\} = -\frac{1}{2}s_r(n). \end{cases} \quad (21)$$

In order to clarify the method, a graphical explanation of the same process is shown in figure 3 using a perfect quadrature signal given by

$$x(t) = D(t) + jQ(t) = (\cos \omega_f t + \sin \omega_r t) + j(\sin \omega_f t + \cos \omega_r t).$$

Here, the spectra of the signals produced at each processing stage in figure 2 are plotted sequentially. In fact, this is a frequency domain description of the frequency shifting and modulation process.

## 2.2. Frequency domain processing

In this section, the Hilbert transform method and complex FFT method will be described. Although the theoretical description of the Hilbert transform method will be entirely based on the time domain expressions, the implementation which is based on the frequency response of the HT given by equation (2) is almost entirely in the frequency domain.

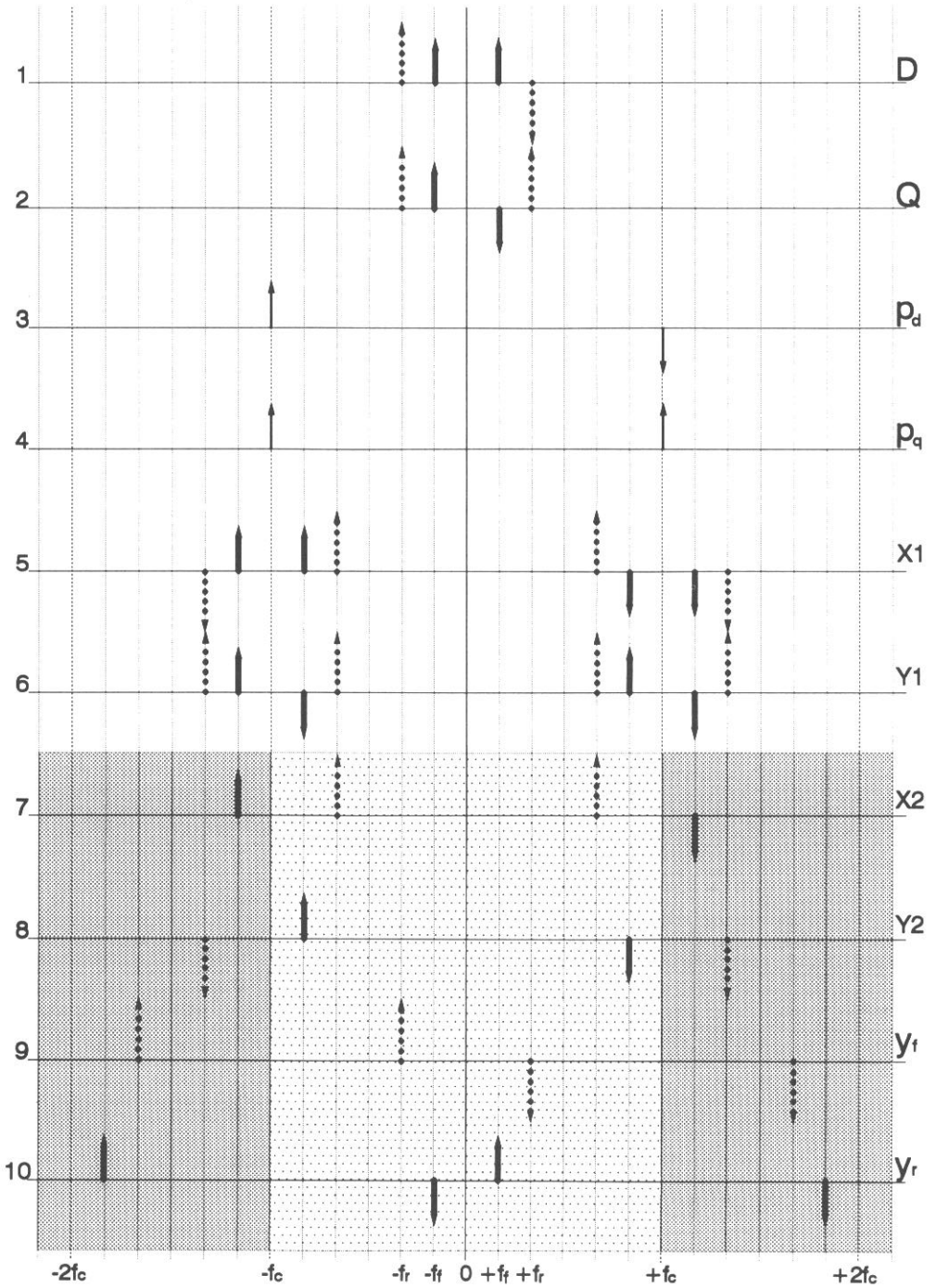
**2.2.1. Hilbert transform method (HTM).** Unlike the phasing filter technique this method utilizes a complex HT in the frequency domain. As outlined in figure 4 the method requires a complex FFT and an inverse FFT (IFFT). The ideal frequency response of the HT given by equation (2) implies that the implementation of the HT is fairly simple in the frequency domain.

To describe the method theoretically, let us consider a Doppler signal defined by equation (1). It can then be shown that

$$s(n) = D(n) + jQ(n) = \{s_f(n) + H[s_r(n)]\} + j\{H[s_f(n)] + s_r(n)\}. \quad (22)$$

Applying the Fourier transform to  $s(n)$ , we have

$$F\{s(n)\} = \{S_f(\omega) + H[S_r(\omega)]\} + j\{H[S_f(\omega)] + S_r(\omega)\}. \quad (23)$$



Lowpass filter cut-off frequency = f<sub>c</sub>, f<sub>c</sub> = f<sub>s</sub>/4

Stop-band region
  Pass-band region

**Figure 3.** Spectra at each processing stage of the EWRT (input signal to be considered  $\cos \omega_r t + \sin \omega_r t + j \sin \omega_f t + j \cos \omega_f t$ ). Spectra indexed by letters on the right-hand-side correspond to the results at each processing stage indexed by the same letters in figure 2.

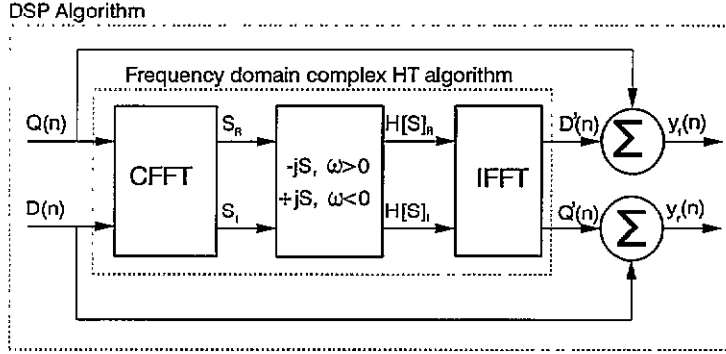


Figure 4. Block diagram of the Hilbert transform method in the frequency domain.

This expression can be rewritten using the definitions given by equations (8), (9), (10), (11), (12) and (13).

$$F\{s(n)\} = S(\omega) = \{S_r^+(\omega) + S_r^-(\omega) - jS_r^+(\omega) + jS_r^-(\omega)\} + j\{-jS_r^+(\omega) + jS_r^-(\omega) + S_r^+(\omega) + S_r^-(\omega)\}. \quad (24)$$

Using equation (2), the HT of equation (24) can be given as

$$H[S(\omega)] = \begin{cases} -jS(\omega) & 0 \leq \omega < \pi \\ +jS(\omega) & -\pi \leq \omega < 0 \end{cases} \quad (25)$$

$$H[S(\omega)] = \{-jS_r^+(\omega) + jS_r^-(\omega) - S_r^+(\omega) - S_r^-(\omega)\} + j\{-S_r^+(\omega) - S_r^-(\omega) - jS_r^+(\omega) + jS_r^-(\omega)\} = \{H[S_r(\omega)] - S_r(\omega)\} + j\{-S_r(\omega) + H[S_r(\omega)]\}. \quad (26)$$

After taking inverse Fourier transform, the HT of the input signal is obtained.

$$F^{-1}\{H[S(\omega)]\} = \{H[s_r(n)] - s_r(n)\} + j\{-s_r(n) + H[s_r(n)]\} = D'(n) + jQ'(n) = H[s(n)] \quad (27)$$

$$D'(n) = H[D(n)] = H[s_r(n)] - s_r(n) \quad (28)$$

$$Q'(n) = H[Q(n)] = -s_r(n) + H[s_r(n)].$$

The final step is to add the complex input signal (equation (1)) and its HT (equation (28)) as depicted in figure 4

$$\begin{cases} y_r(n) = D'(n) + Q(n) = 2H[s_r(n)] \\ y_i(n) = D(n) + Q'(n) = 2H[s_r(n)]. \end{cases} \quad (29)$$

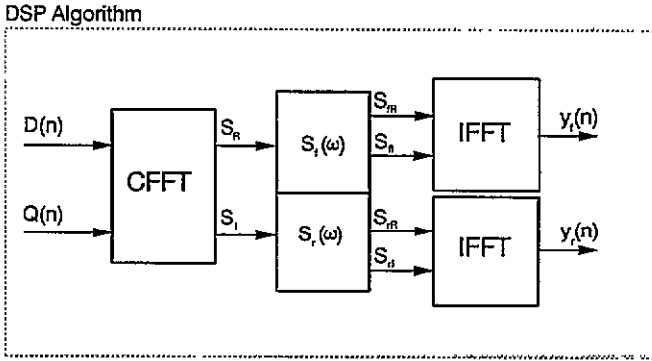


Figure 5. Block diagram of the complex FFT method.

2.2.2. *Complex FFT (CFFT)*. The CFFT has been used to separate the directional signal information from quadrature signals so that spectra of the directional signals can be estimated and displayed as sonograms (Aydin and Evans 1994). Only the magnitude information from the CFFT was however used in that application. It can be proved that the phase information of the directional signals is well preserved and can be used to recover these signals. The method is shown in figure 5.

For a discrete Doppler quadrature signal pair given by equation (1), it can be shown that

$$\begin{aligned}
 D(n) + jQ(n) &= s(n) \\
 &= \{s_f(n) + jH[s_f(n)]\} + \{H[s_r(n)] + js_r(n)\} \\
 &= \{s_f(n) + jH[s_f(n)]\} + j\{s_r(n) - jH[s_r(n)]\}.
 \end{aligned}
 \tag{30}$$

Using the frequency response of the HT given by equation (2), it is easy to obtain the Fourier transform

$$\begin{aligned}
 F\{D(n) + jQ(n)\} &= S(\omega) \\
 S(\omega) &= \begin{cases} 2S_f(\omega) & 0 \leq \omega < \pi \\ j2S_r(\omega) & -\pi \leq \omega < 0. \end{cases}
 \end{aligned}
 \tag{31}$$

It is clear that the positive frequencies of  $S(\omega)$  contain only the spectrum of the forward channel signal  $s_f(n)$ , and its negative frequencies contain only the 90° shifted spectrum of the reverse channel signal  $s_r(n)$ .

If the following spectra are defined

$$S^+(\omega) = \begin{cases} S(\omega) & 0 \leq \omega < \pi \\ 0 & -\pi \leq \omega < 0 \end{cases}
 \tag{32}$$

$$S^-(\omega) = \begin{cases} 0 & 0 \leq \omega < \pi \\ S(\omega) & -\pi \leq \omega < 0 \end{cases}
 \tag{33}$$

using the properties of the Fourier transform, i.e. for a real signal, the real part of its spectrum is an even function, and the imaginary part is an odd one, it is easy to recover the spectra of the two real directional signals. The real part of  $S_f(\omega)$  is

$$\Re\{S_f(\omega)\} = \begin{cases} \Re\{S^+(\omega)\} & 0 \leq \omega < \pi \\ \Re\{S^+(-\omega)\} & -\pi \leq \omega < 0 \end{cases}
 \tag{34}$$

and its imaginary part is

$$\Im\{S_f(\omega)\} = \begin{cases} \Im\{S^+(\omega)\} & 0 \leq \omega < \pi \\ -\Im\{S^+(-\omega)\} & -\pi \leq \omega < 0. \end{cases} \quad (35)$$

The real part of  $S_r(\omega)$  is

$$\Re\{S_r(\omega)\} = \begin{cases} \Re\{S^-(-\omega)\} & 0 \leq \omega < \pi \\ \Re\{S^-(\omega)\} & -\pi \leq \omega < 0 \end{cases} \quad (36)$$

and its imaginary part is

$$\Im\{S_r(\omega)\} = \begin{cases} \Re\{S^-(-\omega)\} & 0 \leq \omega < \pi \\ -\Re\{S^-(\omega)\} & -\pi \leq \omega < 0. \end{cases} \quad (37)$$

The directional time domain outputs can then be obtained by taking the inverse FFTs.

### 3. Simulation study

The four methods described above were simulated in order to compare their relative performances. The simulations were implemented using commercially available digital signal processing software (Hypersignal†) and C language code when a required function was not available in Hypersignal. All the algorithms were applied to the same data set which was a band-limited signal derived from pre-recorded white noise. The record length was 100 frames where each frame consisted of 512 data points. The recorded white noise was filtered by a band-pass filter having 70 dB stop-band attenuation and a reference band-limited quadrature signal was derived from this filtered signal. The complex FFT spectrum of this quadrature signal is shown in figure 6(a). Since the separation level is better than 60 dB, the signal can be assumed to be an ideal quadrature signal.

After obtaining separated signals using each of the four algorithms, a 512 point real FFT preceded by a Hanning window was applied to each of the signals. 50 frames of the FFT results were averaged. The averaged logarithmic power spectra of each signal were then plotted side by side, as if they were a result of the complex FFT (figures 6(b)–(e)).

### 4. Real-time digital implementation of quadrature-to-directional Doppler signal conversion

Figure 7 depicts a general block diagram of the system used. It is based on a DSP board equipped with the AT&T DSP32C (a powerful 32-bit floating point digital signal processor), two AD and DA converters, and an on-board memory. As is necessary for all signal processing systems involving AD and DA conversion, the system includes anti-aliasing and reconstruction filters (Proakis and Manolakis 1992) and the performance of the methods implemented is limited by the specifications of these filters. In order to achieve good separation the specifications of the two anti-aliasing filters must ideally be the same.

The board has an interface to communicate with the host computer. The program running on the DSP chip can be manipulated via this interface.

† Hyperception, Inc., 9550 Skillman LB125, Dallas, TX 75243, USA.

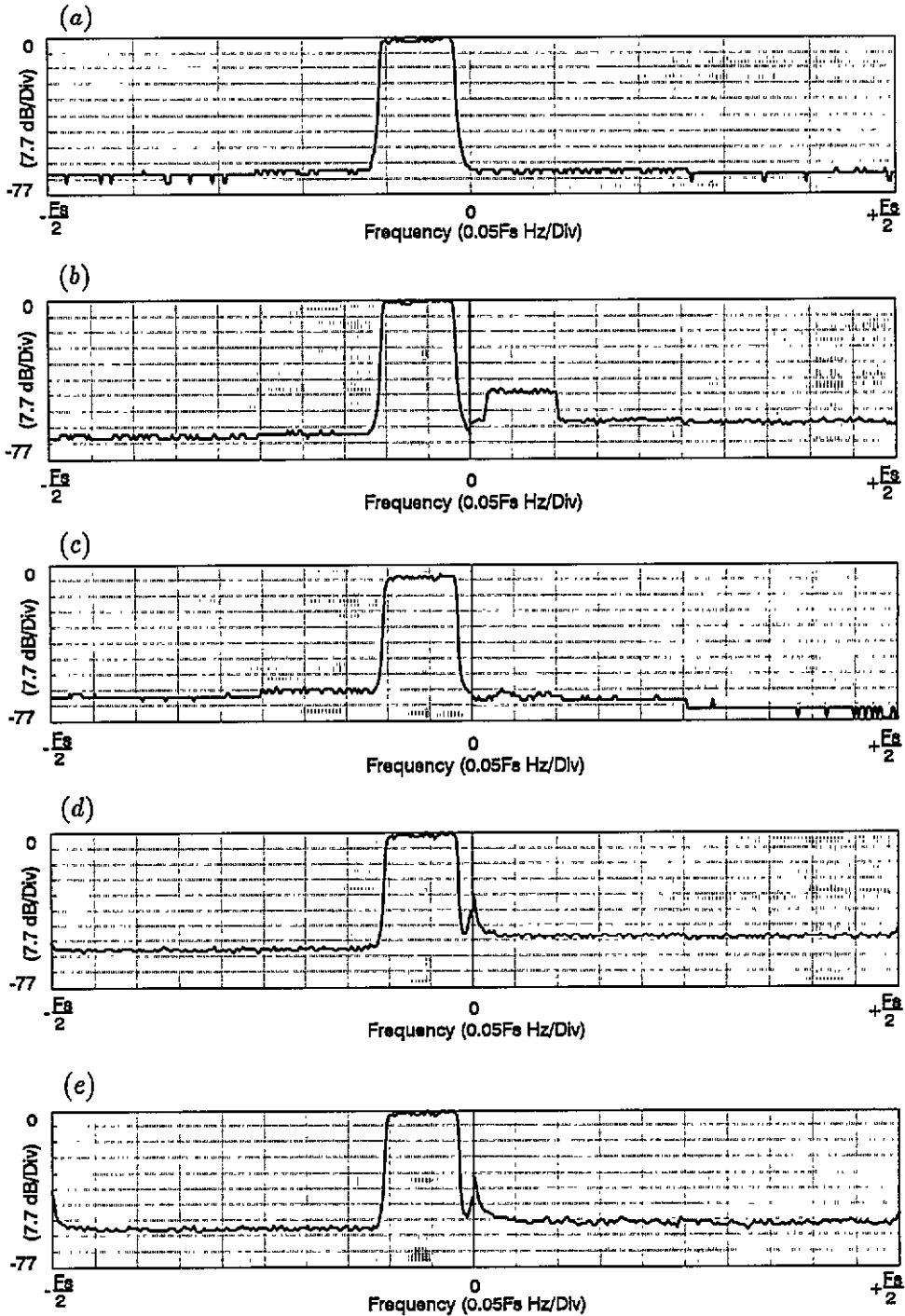


Figure 6. The averaged output power spectra of the simulations for, (a) the reference quadrature signal, (b) PFT, (c) EWRT, (d) HTM and (e) CFFT.

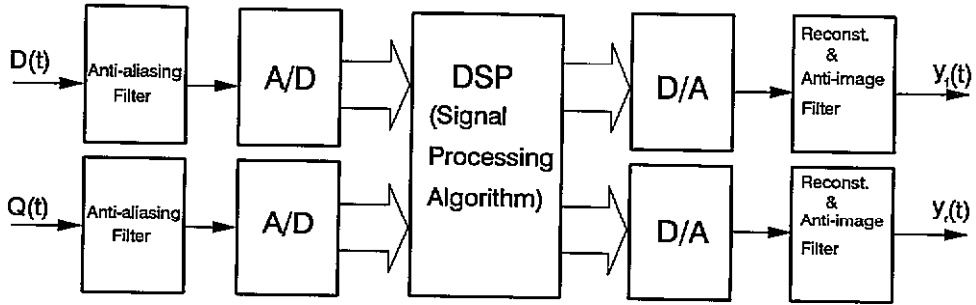


Figure 7. General quadrature-to-directional format conversion system block diagram.

The basic operation of the algorithm for all the proposed methods is to convert the analogue quadrature data into digital form, store it in the DSP board's memory, process it, and finally convert the digital data back into analogue signals. The outputs of the system are totally separated and ready to be recorded without suffering from phase distortion.

In order to verify these implementations, a continuous narrow-band quadrature pair signal containing components corresponding to both directions was used. For this purpose the output of a wide-band analogue white-noise generator was digitized and digitally filtered to give two different narrow-band signals. The filtered signal was processed according to equation (1) to produce a quadrature pair, and then the digital quadrature signals were converted to analogue form via the DA converters. The complex FFT spectrum of this quadrature pair is illustrated in figure 8 where the narrow-band signals occupy different frequency ranges and correspond to opposite directions of flow. This quadrature signal was processed using each of the methods described and the separated channels were recorded on digital audio tape in real time. These results were monitored on a dual-channel spectrum analyser by replaying the recordings. The intermediate recording stage was necessary as the same computer system was used both for the real-time processing and as a dual-channel spectrum analyser.

#### 4.1. Implementations of time domain processing

In this section practical algorithms for the time domain processing will be presented and alternative implementations mentioned.

Although a data length of  $2^n$  points was used in the implementation described here, this is not obligatory for time domain processing, and any data length satisfying real-time processing conditions can be used.

**4.1.1. Implementation of phasing filter technique.** Since a detailed explanation on this method has been given in a previous paper (Aydin and Evans 1994), only a brief description of the implementation is given here.

As depicted in figure 1, this method is based on a digital HT. The HT of a band-limited signal can be obtained by convolving this signal with the impulse response of the HT given by equation (3), which is purely a time domain process. Digital implementation of the HT can be achieved most readily using finite impulse response (FIR) techniques (Rabiner and Schafer 1974, Bateman and Yates 1988).

In this algorithm, improved specifications of the HT leads to an improved separation level. However, this improvement is limited by the DSP microprocessor speed. Figure 9 shows impulse, frequency and phase responses of the HT used in the actual implementation.

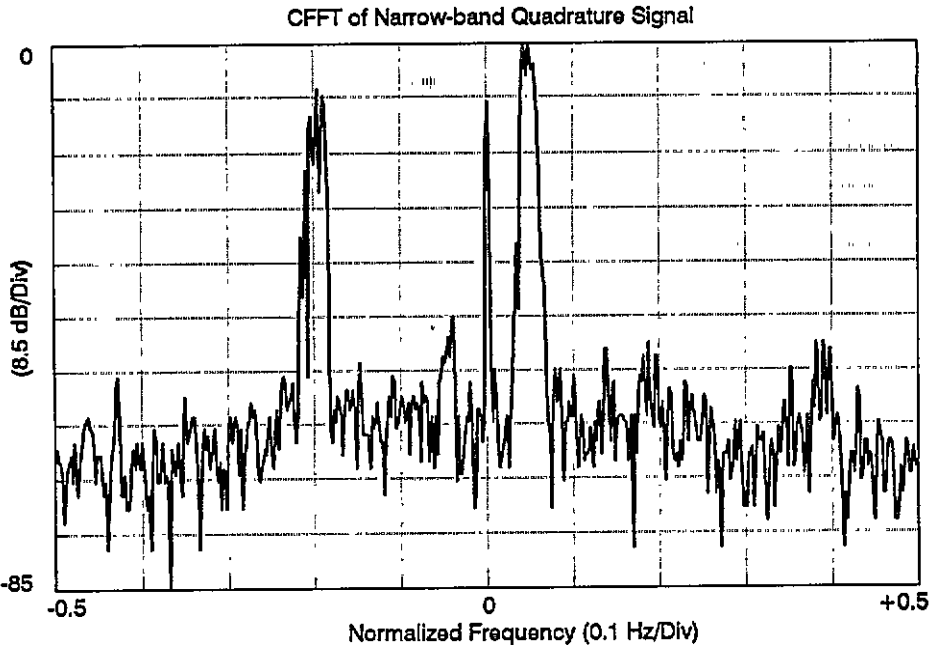


Figure 8. Complex FFT spectrum of narrow-band quadrature test signal.

When the narrow-band quadrature signal described above is applied to this system, the results are as illustrated in figure 13(a) below.

An alternative algorithm is to implement the HT using recursive networks which are basically phase splitters (Gold *et al* 1970, Ansari 1987). A  $90^\circ$  phase splitter is an all-pass filter which produces a quadrature signal pair from a single input as illustrated in figure 10. Since IIR filters require less coefficients than FIR filters, this implementation can reduce the processing time.

*4.1.2. Implementation of extended Weaver receiver technique.* Implementation of the EWRT is as described by Aydın and Evans (1994) up to the stages X2 and Y2 (figure 2). That is to say, a quadrature pilot frequency signal having a frequency of  $f_s/4$  was generated and mixed with the incoming quadrature Doppler signal as previously described. The signals at these stages are SSB modulated. The upper side-bands are removed by the low-pass filters. After filtering the forward and reverse signals are already separated, but are still modulated with the pilot frequency and so they must be translated down to base-band. The second mixing stage implements this translation as explained above. The outputs of the mixers contain higher frequency signals as well as base-band signals, so the higher frequency components are filtered out by the last filtering stage.

Since a linear phase response is not required, the filters were implemented using IIR structure which enabled the design of faster filters. The cut-off frequency of the filters must be equal to the pilot frequency signal. The transition bandwidth should be kept as narrow as possible. As an example, in our implementation the low-pass filters provide at least 40 dB attenuation at a frequency of  $(f_s/4) + (f_s/400)$ .

In this particular application the sampling frequency was set to be 40.96 kHz and the frequency of the pilot frequency signal and filter cut-off frequencies were 10.24 kHz. The

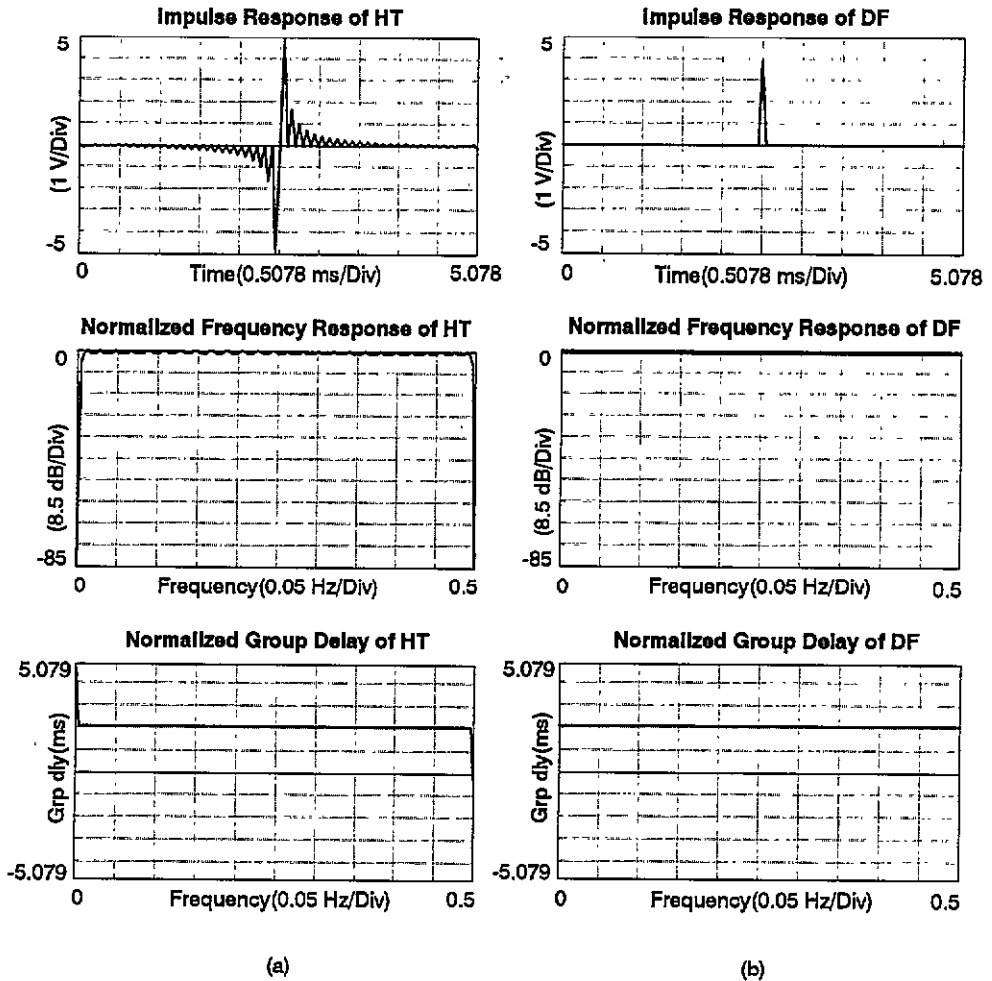


Figure 9. Impulse, frequency and phase responses of (a) the Hilbert transform and (b) delay filters with 105 taps.

normalized frequency response of a 12th-order elliptical low-pass filter which is used in the implementation is shown in figure 11. Notice that the decline of the frequency response is extremely sharp. This would not have been possible with analogue processing.

The spectra of the directional signals produced by the EWRT are illustrated in figure 13(b) below.

An alternative algorithm utilizing two quadrature mixers instead of one is given in figure 12, because of the pipelined architecture of the DSP32C two extra multiplications do not affect the execution speed of the algorithm.

#### 4.2. Implementations of frequency domain processing

As their name implies, these signal processing functions are performed in the frequency domain. The common step for all such frequency domain processing methods is the FFT which uses a data length defined by  $2^n$ , where  $n$  is the FFT order. It should be pointed out

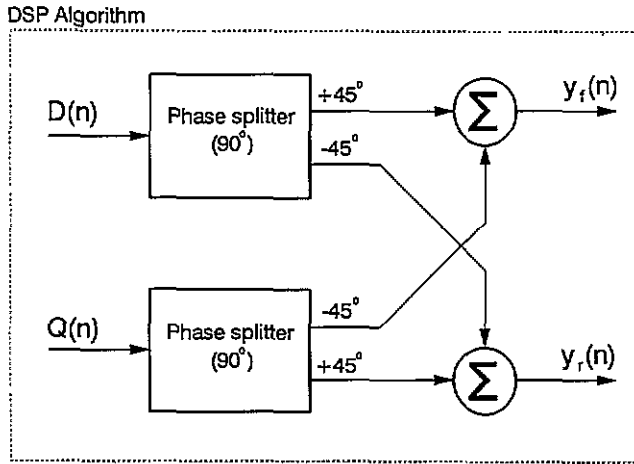


Figure 10. Alternative implementation of the FFT using phase splitters.

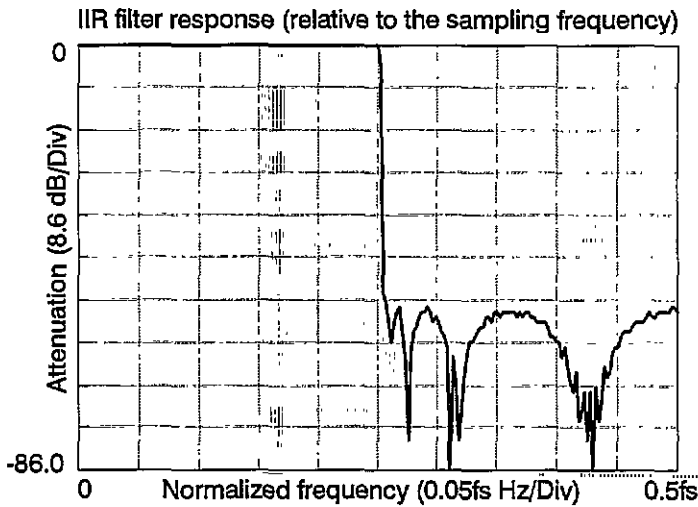


Figure 11. Normalized frequency response of the 12th-order IIR low-pass filter used in the EWRT.

that overlap techniques should be used in these methods to avoid discontinuities caused by the edge effects (Oppenheim and Schaffer 1975, Harris 1982). The performance of these systems is limited by the FFT resolution.

*4.2.1. Implementation of Hilbert transform method.* The implementation of the HTM is based on equation (2) which is the ideal frequency response of the HT. An  $M$  element complex discrete time domain signal array must be converted into the frequency domain using an  $N$ -point CFFT, where  $N$  must be greater than  $M$  to use overlap techniques as mentioned above.

The complex FFT result is a complex frequency domain signal containing real and imaginary parts where the phase information is preserved. Applying equation (2) to this frequency domain signal as illustrated in figure 4 produces a complex frequency domain

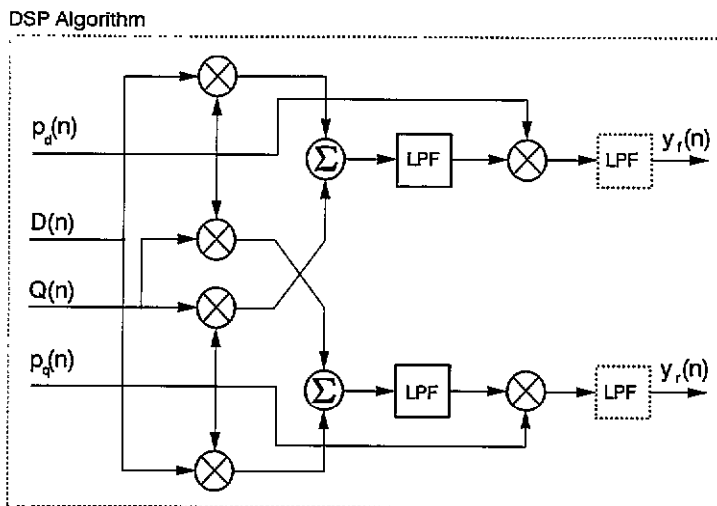


Figure 12. Alternative EWRT algorithm using two image reject mixers.

signal which is equal to the complex FFT of the HT of the original input signal. The IFFT of the new frequency domain signal gives the HT of the input complex discrete time domain signal. After scaling, simple additions give the separated outputs.

The response of the system when the narrow-band quadrature signal is applied to it is shown in figure 13(c) below.

An alternative implementation of the HT is to use multiplication in the frequency domain instead of the time domain convolution employed in the PFT. This is performed by taking the FFT of the FIR HT filter once and storing the result. Then, this result and the complex FFT of the input signal are multiplied to produce the complex FFT of the HT of the input signal. After that the same process as described above is performed.

4.2.2. *Implementation of complex FFT.* The implementation of this method is straightforward, but overlapping processing is necessary in practice to overcome the discontinuity problem caused by data segmentation. The real-time implementation steps can be summarized as follows:

- (i)  $N/4$  points of data are captured from each channel ( $D$  and  $Q$ ) by the AD converters;
- (ii) these data are added to  $3N/4$  points of the most recent data to obtain an overlapped  $N$ -point data block for each channel;
- (iii) the two  $N$ -point data blocks are taken as the real and imaginary input parts to calculate the complex FFT;
- (iv) with the complex FFT results (equation (31)), the necessary processing (equations (32)–(37)) is done to separate the information of forward and reverse channels;
- (v) two  $N$ -points inverse FFTs are calculated using equations (34) and (36) and equations (35) and (37) as the real and imaginary parts, respectively;
- (vi) the middle  $N/2$  points data of each of the inverse FFTs are output to a DA converter so that there is no discontinuity in the output signals;
- (vii) the processing from step (1) is repeated until an interruption is received.

The steps in (i)–(vii) do not represent the time sequence of the implementation. For

example, the input of the quadrature signals, the output of the directional signals and the calculation of the FFTs are carried out simultaneously in practice.

The output spectra of the system for the quadrature narrow-band signal described above are shown in figure 13(d) below.

## 5. Results

### 5.1. Simulation results

The simulation results are shown in figure 6. Figure 6(a) is the reference quadrature signal spectrum. Figure 6(b) are the averaged power spectra of the separated channels plotted side by side for the PFT. Here, the cross-talk level is approximately  $-45$  dB. The level of the cross-talk depends on the HT filter characteristics. A reduction in pass-band ripple and an increase in stop-band attenuation result in a decrease in the cross-talk. However, this will increase the length of the filter, i.e. its execution time. This problem is associated with FIR-type Hilbert transform implementations. If a  $90^\circ$  phase splitter is used this problem can be avoided.

The result of the EWRT is illustrated in figure 6(c), where the separation level is approximately  $-55$  dB. In the EWRT the separation level is a function of the quadrature pilot frequency signal. The best performance is obtained for a quadrature pilot signal frequency of  $f_s/4$  when the look-up table method is used.

The frequency domain methods (figures 6(d) and 6(e)) produce almost the same separation levels ( $\approx -50$  dB). The main drawback of these methods is the discontinuities caused by the data segmentation. Although this effect is minimized by using an overlapping technique, these methods corrupt the output signal with a very low frequency signal. However, since the level of this signal and its harmonics are usually less than  $-30$  dB, this effect is negligible.

### 5.2. Practical results

The theoretical derivation of the separated time domain signals from a band-limited quadrature signal has been verified by practical implementation. It has been shown that DSP methods make it possible to implement techniques such as EWRT and CFRT to obtain the separated time domain outputs in real-time. All the methods are able to process Doppler signals with frequencies of up to 15 kHz when a DSP board based on the AT&T DSP32C DSP microprocessor is used as the processing platform. Although the execution times may be decreased by optimizing the DSP code, the real-time execution speeds of our implementations are summarized in table 1.

**Table 1.** The approximate cross-talk rejection levels and real-time execution times of the algorithms.

Method	Data length	Sampling frequency (kHz)	Execution time (ms)	Separation level <sup>a</sup> (dB)
EWRT	512	40.96	7.5	$-55$
PFT	256	20.48	8.9	$-45^b$
CFRT	256	20.48	8.5	$-52$
HTM	256	20.48	9.5	$-50$

<sup>a</sup> Simulation results.

<sup>b</sup> Depends on the HT filter specification.

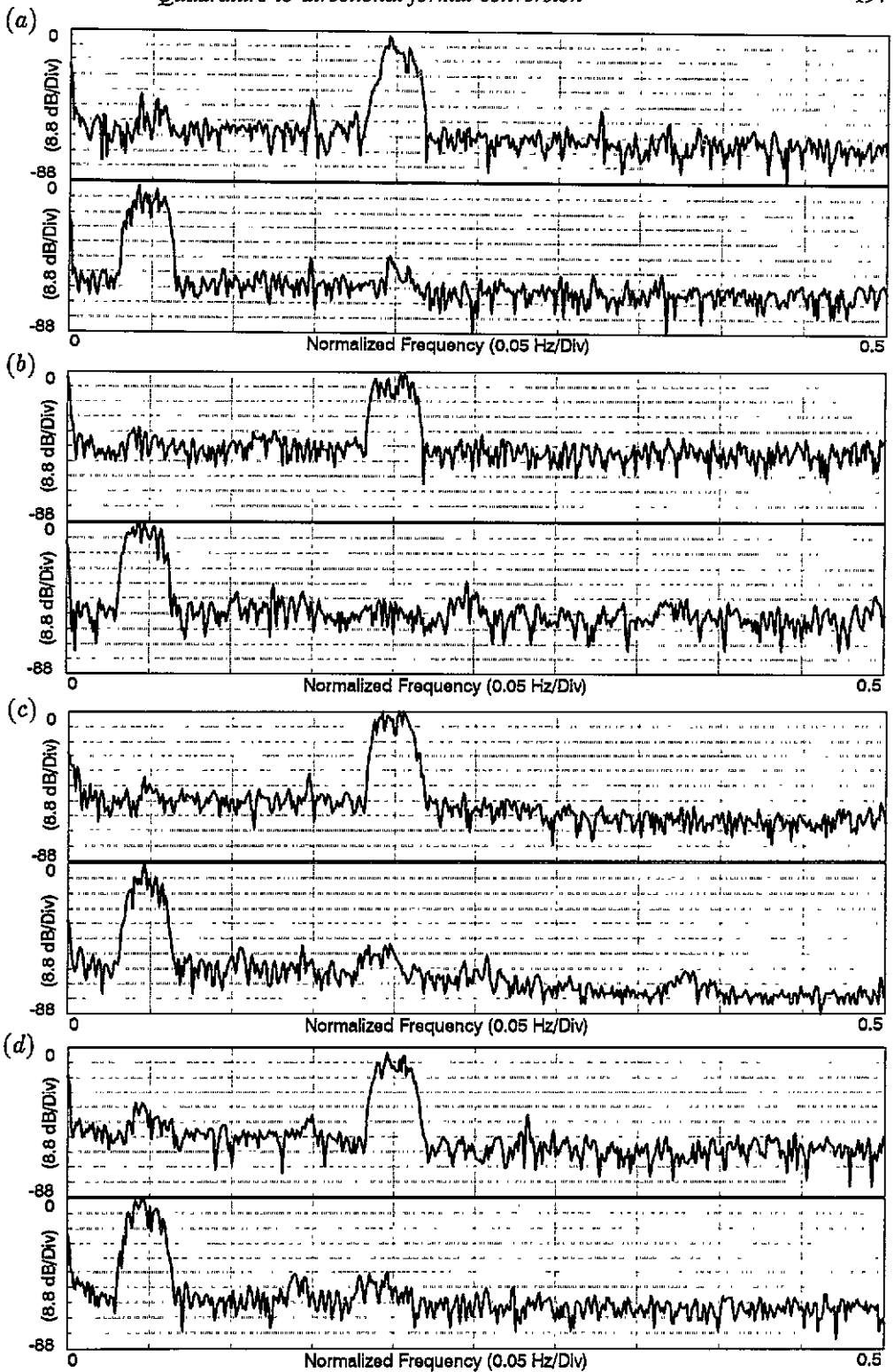


Figure 13. Logarithmic scale output spectra of practical implementations for, (a) PFT, (b) EWRT, (c) HIM and (d) CFFT.

A narrow-band quadrature noise signal containing components representing both flow directions was used to test the methods by first recording the separated outputs on a stereo tape, then playing them back and observing them on a dual-channel spectrum analyser (real-time spectrum analyser option of the Hypersignal DSP software). Examples of the spectra of the signals produced by the four systems for different data segments are illustrated in figure 13.

## 6. Discussion and conclusion

The performances of all the methods described in this paper are very similar. In fact, since floating point DSPs offer the implementation of near ideal systems, the limitations of the performances of these digital techniques are defined by external conditions such as the reconstruction and anti-aliasing filters and AD converter resolution.

The FFT is based on a time domain HT which is implemented using an FIR-type filter. The main limitation of this method is the bandwidth of the filter response. The separation level can be increased by increasing the filter specifications, but this will cause an increase in the execution time of the system. Since this method implements a time domain convolution, the input data length has not necessarily to be fixed.

The EWRT utilizes modulation techniques. In this method, the input signal must be band-limited to  $f_s/4$  for the reasons given above. The performance of the system also depends on the accuracy of the quadrature pilot frequency. Only one real FFT is required to display the separated frequency domain signals while it outputs totally separated time domain signals.

The performances of frequency domain processing methods based on the applications of the FFT properties rely entirely on the FFT resolution. Using larger FFTs leads to finer resolution results. However, the discontinuities caused by the Gibbs phenomenon (Proakis and Manolakis 1992) must be avoided by applying overlapping or zero-padding techniques. This implies that the FFT length must be longer than the input data length.

The results of the simulations show that the cross-talk rejection for all the methods is greater than 40 dB. This is summarized in table 1. The EWRT provided the best cross-talk rejection and also gave the fastest execution time. For the frequency domain display it requires only one real FFT. However, the Doppler signal must be band-limited to  $f_s/4$ . This implies that the required memory space to record a digitized quadrature Doppler signal is twice that required by the other methods. When a floating point processor is used this appears to be the best method.

The PFT is more suitable for fixed-point processors since it employs FIR-type filters. It also requires less memory to record the quadrature Doppler signal. Since the performances of frequency domain methods (HTM and CFFT) are a function of the FFT length, it is better to use them with fast processors to implement higher resolution complex FFT.

Although there are minor differences between the performances of the four algorithms, the simulated and practical results show that all the methods give satisfactory results, so the method of choice will depend on the details of the implementation platform.

## Acknowledgment

This work supported in part SERC grant GR/G00 372 and the Turkish Ministry of Education.

**References**

- Ansari R 1987 FIR discrete-time Hilbert transformers *IEEE Trans. Acoust., Speech, Signal Processing ASSP-35* 116-19
- Aydin N and Evans D H 1994 Implementation of directional Doppler techniques using a digital signal processor *Med. Biol. Eng. Comp.* at press
- Bateman A and Yates W 1988 *Digital Signal Processing Design* (London: Pitman) pp 279-332
- Bush G and Evans D H 1993 Digital audio tape as a method of storing Doppler ultrasound signals *Physiol. Meas.* 14 381-6
- Cizek V 1970 Discrete Hilbert transform *IEEE Trans. Audio Electroacoust. AU-18* 340-3
- Coghlan B A and Taylor M G 1976 Directional Doppler techniques for detection of blood velocities *Ultrasound Med. Biol.* 2 181-8
- Gibson J D 1989 *Principles of Digital and Analog Communications* (New York: Macmillan) pp 113-18
- Gold B, Oppenheim A V and Rader C M 1970 Theory and implementation of discrete Hilbert transform *Proc. Symp. Comput. Process. Comm.* (New York: Polytechnic Press) pp 235-50
- Harris F J 1982 The discrete Fourier transform applied to time domain signal processing *IEEE Communication Magazine* 20 13-22
- Oppenheim A V and Schaffer R W 1975 *Digital Signal Processing* (Englewood Cliffs, NJ: Prentice-Hall) pp 110-5 and pp 337-66
- Proakis G P and Manolakis D G 1992 *Digital Signal Processing. Principles, Algorithms, and Applications* (New York: Macmillan) pp 169, 411 and 585
- Rabiner L R and Schaffer R W 1974 On the behaviour of minimax FIR digital Hilbert transformers *Bell System Tech. J.* 53 363-89
- Schwartz M, Bennett W R and Stein S 1966 *Communication Systems and Techniques* (New York: McGraw-Hill) pp 29-35
- Smallwood R H 1985 Recording Doppler blood flow signals on magnetic tape *Clin. Phys. Physiol. Meas.* 6 357-9